ISBN: 978-3-95450-227-1 ISSN: 2673-5490 doi:10.18429/JACoW-IPAC2022-TUPOTK025

DESIGN STUDY OF THE THIRD HARMONIC SUPERCONDUCTING CAVITY FOR A BUNCH LENGTHENING

J. Yoon[1,2], E. S. Kim*[1], J. Han[2], H. S. Park[2], E. Kako[3]
[1]Dept. of Accelerator Science, Korea University, Sejong, South Korea
[2]Kiswire Advanced Technology Ltd, Daejeon, South Korea
[3]High Energy Accelerator Research Organization (KEK), Tsukuba, Japan

Abstract

The bunch lengthening by the 3rd harmonic cavity reduces the electron collisions in a bunch and increases the Touschek lifetime of a storage ring. We performed the multiphysics simulations including the electromagnetic, thermal, and mechanical analysis of the cavity. In the electromagnetic simulation, the geometry is optimized for the required performance of the cavity. The elliptical double-cell geometry is selected to increase the accelerating voltage and reduce the power losses of the cavity. Thermal/mechanical analyses were performed to check the deformation of the thermal and pressure contraction. The prototype cavity does not require the power coupler as it is a passive type. The conceptual design and copper prototype of the 3rd harmonic cavity will be described in this paper. Based on this design, the fabrication of Niobium cavity is in progress.

DESIGN REQUIREMENTS

The design requirements of the cavity are shown in Table 1. The resonant frequency (f_{res}) of the 3rd harmonic cavity is 1499.631 MHz as the frequency of the main cavity is 499.877 MHz. The main features are a passive type and superconductor. In the case of a passive cavity, it can be operated without a power coupler.

Table 1: Design Requirements of the 3rd Harmonic SRF Cavity

Parameter	Value
f_{res}	1499.631 MHz
Type	Passive, Superconductor
RF voltage	800 kV
$(R/Q)_{\text{per cell}}$	90 Ω

The shunt impedance divided by the unloaded quality factor (R/Q) is calculated by Eq. (1) [1]. Since the beam current and accelerating voltage of the cavity are 400 mA and 800 kV, the R/Q and δf (detuning frequency) is calculated as 90 Ω and 69.5 kHz.

$$V = I_b\left(\frac{R}{Q}\right)_{\text{per cell}}\frac{f_0}{\delta f} \tag{1}$$

* eskim1@korea.ac.kr

ELECTROMAGNETIC DESIGN

Basic Geometry and Parameter Sweeping

The basic geometry of the 3rd harmonic superconducting cavity (HSC) is adopted as an elliptical cavity. The 3rd HSC has relatively low accelerating voltages and gradients. Therefore, we chose the low loss geometry to minimize the power loss of the cavity [2].

Figure 1 shows variations of the shunt impedance divided by unloaded quality factor due to the changes in the bore radius. If the bore radius changes, the diameter of the cavity also changed for the target resonant frequency. Therefore, the horizontal axis is expressed as a ratio of radius and diameter. We can reach the R/Q to 90 Ω by the adjustment of a ratio of the cavity. However, the strength of higher-order modes (HOM) are not negligible [3]. Therefore, we will suppress it with HOM absorbers and design progress is ongoing.

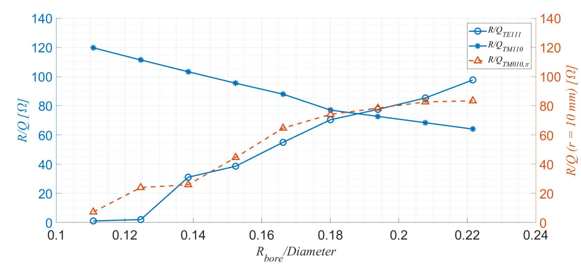

Figure 1: R/Q variations due to the bore diameter.

Number of Cells

Figure 2 shows the geometry of the cavities, and the main parameters are listed in Table 2. The double-cell geometry can reach the required accelerating voltage at lower accelerating gradient. This geometry has also a lower strength of the surface magnetic field compared to the single cell.

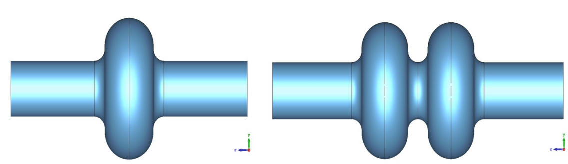

Figure 2: Geometry of the cavity: (left) Single-cell and (right) Double-cell.

Lorentz Force Detuning

The electromagnetic field induces the surface current on the wall of the cavity. For this reason, the Lorentz pressure

ISBN: 978-3-95450-227-1 ISSN: 2673-5490 doi:10.18429/JACoW-IPAC2022-TUPOTK025

Table 2: Performance of the Cavities

Parameters	Single cell	Double-cell
Resonant frequency	1499.631 MHz	1499.647 MHz
$E_{\text{peak}}/E_{\text{acc}}$	2.07	2.23
$H_{\text{peak}}/E_{\text{acc}}$	4.08 mT/(MV/m)	
R/Q	95.7 Ω	190.8 Ω
Required V_{acc}	800 kV	
E_{acc} in operation	8 MV/m	4 MV/m
B_{peak} in operation	32.5 mT	16.35 mT

is also generated on the surface of the cavity. Therefore, the coefficient of the Lorentz force detuning (LFD) is related to the accelerating field and frequency shift. ($\Delta f \propto k_L E_{acc}^2$) [4]. The results of the LFD analysis with the fixed beam tube are listed in Table 3. The presence of the stiffener decreases the effect of the Lorentz force. Therefore, we add the stiffener between the cells for the stability of the cavity.

Table 3: Lorentz Force Detuning Factor (k_L) and Deformation

Status	k_L $[Hz/(MV/m)^2]$	Max. Deform [mm]
w/o stiffener	-7.26	1.59×10^{-5}
w/ stiffener	-3.52	8.12×10^{-6}

THERMAL/MECHANICAL ANALYSIS

Thermal and Pressure Contraction

The operating temperature of the 3rd HSC is 4.5 K for the superconducting state. Moreover, the inside of the cavity is a vacuum status to reduce obstruction of beam acceleration. Therefore, the thermal/pressure contraction occurs due to the low temperature/vacuum pumping, respectively. In this case, the deformed geometry affects the resonant frequency of the cavity. The results of the deformation by the contraction are listed in Table 4.

Table 4: Thermal/Pressure Contraction

Cause of deform.	Δf [kHz]	Max. Deform. [mm]	Max. Stress [MPa]
Temperature (293 K to 4.5 K)	-2126.22	0.337	5.51×10^-4
Pressure (atmosphere to vacuum)	-35.24	4.48×10^-3	6.96

The maximum stress is under the allowable peak stress of Niobium [5]. However, the difference in the resonant frequency is -2.13 MHz due to thermal contraction, which is bigger than pressure contraction. The results of the deformation indicate that the effect of the contraction and volume change due to buffered chemical polishing (BCP) should be considered. Therefore, we calculate the target frequency of the cavity geometry after the electron beam welding, and the results are listed in Table 5. Our target frequency of the cavity at room temperature is confirmed to be 1500.455 MHz.

Table 5: Frequency Tuning Table

	Process	$\Delta f[kHz]$	$f_\pi[MHz]$
0	Operation (4.5 K)	N/A	1499.631
1	Cool down (293 K to 4.5 K)	-2126.22	1497.505
2	Vacuum pumping (0.13 MPa)	-35.24	1497.469
3	BCP (200 µm)	2985.88	1500.455

RF MEASUREMENTS AT ROOM TEMPERATURE

Half-cell

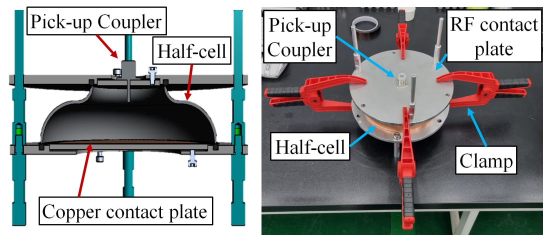

Figure 3: The set-up status of the RF measurement for a half-cell.

Figure 3 shows the RF measurement set-up for a copper half-cell. Copper contact plate increases the RF contact surface due to the small errors at the surface of the fabricated model [6]. From this measurement, we find the frequency sensitivity of the remaining length at the equator section of a half-cell. Figure 4 shows the frequency variation due to the changes in the remaining length. In the case of the presence of the frequency errors in a half-cell, we can adjust the resonant frequency of a half-cell by trimming the equator section.

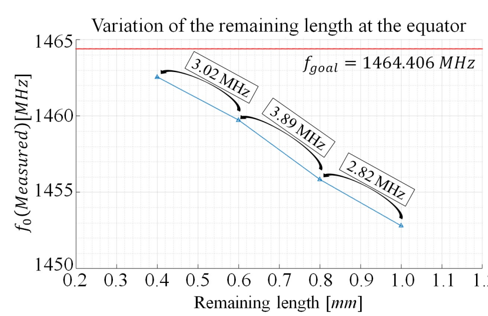

Figure 4: The effect of the trimming length of a half-cell.

Dumbbell

In the case of the dumbbell, the resonant frequency is detected as combined of each half-cell. Therefore, we use the perturbation tip to check the resonant frequency of the

ISBN: 978-3-95450-227-1 ISSN: 2673-5490 doi:10.18429/JACoW-IPAC2022-TUPOTK025

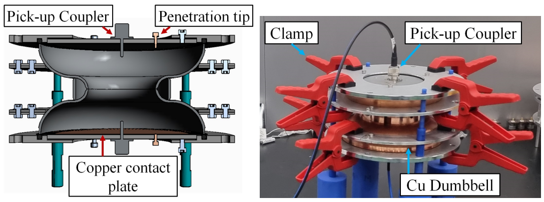

Figure 5: The set-up status of the RF measurement for the dumbbell.

individual half-cells [7]. Figure 5 shows the RF measurements set up for a copper dumbbell and the results of the measurement are listed in Table 6. In the case of dumbbell number 2, the difference in each half-cell is bigger than that of dumbbell number 1. However, the difference and error of the perturbed frequencies are 813 kHz and 0.05 %, respectively. Therefore, we fabricate the dumbbells to copper cavities.

Table 6: Unperturbed (f_π) and Perturbed ($f_{p,l,\pi}$ and $f_{p,r,\pi}$) Frequencies of Each Dumbbell

Parts	f_π [MHz]	$f_{p,l,\pi}$ [MHz]	$f_{p,r,\pi}$ [MHz]	Δf ($f_{p,l,\pi}$-$f_{p,r,\pi}$)
No. 1	1504.642	1504.073	1504.277	-0.204
No. 2	1504.325	1503.013	1502.2	0.813

Copper Cavity

Figure 6 shows the fabricated copper cavity and the bead pull test bench. Copper cavities were fabricated by the Kiswire Advanced Technology (KAT). We chose the cylindrical type of bead, and the diameter and length are the same as 8 mm. In the case of the 8 mm bead, the difference in the resonant frequency is 0.8 MHz. We also set up the tuning plate to adjust the resonant frequency of each cell. The role of the end plates is the adjustment of the center of a bead.

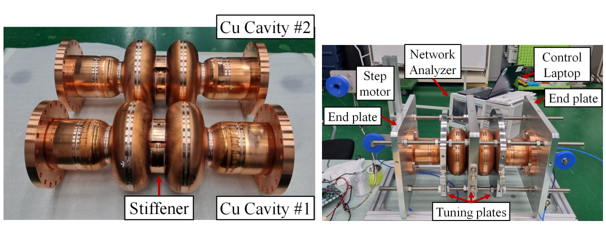

Figure 6: (Left) the fabricated copper cavity and (Right) the bead pull test-bench.

Figure 7 shows the results of the bead pull test. The field flatness of each cavity is 97.25 % and 96.7 %. The reason for the low field flatness of the copper cavity number 2 is an imbalance of the resonant frequency of a dumbbell. However, It is expected that an imbalance of cells can reduce by tuning procedures.

CONCLUSION

The 3rd harmonic superconducting cavity is designed to improve the performance of the 4th generation storage

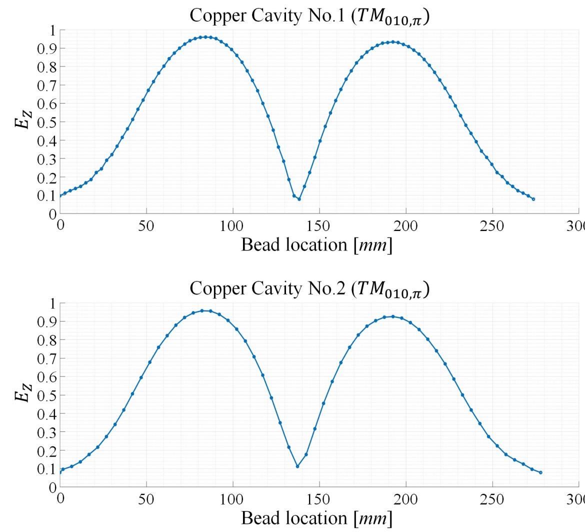

Figure 7: The results of the bead pull test: (Up) copper cavity No.1 and (Bottom) copper cavity No. 2.

ring. The cavity is based on an elliptical and a passive type, which has a simple shape compared to an active type due to absence of power couplers. Electromagnetic design and thermal/mechanical analysis were performed to derive an optimum geometry. We fabricate copper cavities to check fabrication processes and test procedures at room temperature. The field flatness of copper cavities is 97 % without tuning process. A futher review for the fabrication of a Niobium cavity is in progress, and the vertical test is scheduled for the end of 2022.

REFERENCES

[1] Eun-San Kim, "Analysis on Control of the Bunch Length by Passive Harmonic RF Cavities in Storage Rings", *Journal of the Korean Physical Society*, vol. 53 no. 4, pp. 1866-1871.

[2] J. K. Sekutowicz, "Superconducting elliptical cavities", presented at the CAS-CERN Accelerator School: Specialized Course on RF for Accelerators, Jun. 2010, Ebeltoft, Denmark.

[3] F. Marhauser, Higher Order Modes (HOMs). `https://indico.jlab.org/event/98/contributions/7448/attachments/6309/8357/4T-HOMs.pdf`

[4] J. L. Munoz and F. J. Bermejo, "Lorentz Force Detuning Simulations of Spoke Cavities With Different Stiffening Elements", in *Proc. SRF'13*, Paris, France, Sep. 2013, paper THP024.

[5] H. Zheng *et al.*, "Design Optimization of a Mechanically Improved 499.8-MHz Single-Cell Superconducting Cavity for HEPS", *in IEEE Transactions on Applied Superconductivity*, vol. 31, no. 2, Mar. 2021, p. 3500109.

[6] J. Iversen *et al.*, "Development and Design of a RF-Measurement Machine for the European XFEL Cavity Fabrication", in *Proc. SRF'09*, Berlin, Germany, Sep. 2009, paper THPPO071, pp. 786–790.

[7] Sun An *et al.*, "A method to measure the frequencies of individual half cells in a dumbbell cavity", *Rev. Sci. Instrum.*, vol. 79 no. 10, p. 104701, Oct. 2008. doi:10.1063/1.2987686